

Incompletely ordered phases and phase transitions in the three-dimensional general clock model

Yohtaro Ueno and Katsumi Kasono

Department of Physics, Tokyo Institute of Technology, Oh-okayama, Meguro, Tokyo 152, Japan

(Received 17 February 1993; revised manuscript received 28 July 1993)

In our previous studies of the antiferromagnetic Potts and $Q=6$ clock models in three dimensions, we have argued the existence of an incompletely ordered phase (IOP) which is characterized by soft rigidity with a nonintegral stiffness exponent and an incomplete order (though long ranged) such that some of the spin states are exclusively dominant. To investigate the IOP's further, we study Q -state general clock models with one varying energy parameter which can include the ferromagnetic Potts models, by means of our Monte Carlo twist method and analytically in the pair approximation. The twist method gives the following results for $Q=6$. There are two kinds of IOP's (IOP1 and IOP2) on the opposite side of the ferromagnetic Potts model. Their stiffness exponents are about 1.2 less than 2 (for the highest rigidity) in good agreement with those previously obtained. A pair of adjacent clock states are dominantly well mixed in the IOP1, as are a set of three adjacent ones in the IOP2. Thermal fluctuations in the IOP's can be characterized by the spin configurations of the soft structures with buffers that prevent spins in different states by more than the least angle from getting with each other, which is consistent with the nonintegral stiffness exponent. Large entropy contributions to the IOP's are revealed in both approaches. The phase boundary, which extends from the ferromagnetic Potts point, is clearly of first order, while among those relevant to the IOP's one is discontinuous and the other is continuous but the last two are not evident. It is strongly suggested that there is a transition without symmetry breaking between the IOP2 and the rigid phase. In the pair approximation applied for $Q=4\sim 12$, various properties for $Q=6$ are consistent with those obtained by the simulation, except some other properties. Peculiar Q dependence of the highest critical temperature of the IOP in the extreme case is also found.

I. INTRODUCTION

There has been considerable interest in three-dimensional (3D) highly degenerate systems of classical spins that have nonzero ground-state entropy per spin. Problems on their phase transitions seem very profound, but still little has been resolved. The pure Q -state antiferromagnetic (AF) Potts models¹ are the simplest of such systems. Among the Q different relative spin states of a pair of nearest-neighbor spins in these models, $Q-1$ are at the lowest-energy level, while one is at the highest. This is in contrast to the ferromagnet case in the inverse situation. Thus, there are lots of possibilities to make those states connect into a network, causing high degrees of degeneracy in the ground state. Then it is natural to expect a distinct kind of phases if there are phase transitions and to get interested in the role that entropy should play in the mechanism of ordering as Berker and Kadanoff initiated a study in this direction.² The purpose of the present paper is to pursue such interest in the general clock (GCL) models, following the previous studies of the AF Potts models³ and the ordinary six-state clock model in $D=3$.⁴ In the previous work we have argued for the existence of a novel type of ordered states, which we call *incompletely ordered phases* (IOP). By means of our Monte Carlo (MC) twist method and the pair approximation, we shall make an extensive study of the IOP's and their related phase transitions in the GCL models.

Berker and Kadanoff conjectured, in such highly degenerate systems, a distinct phase where correlations decay algebraically with distance.² However, later studies

on the 3D AF Potts models disagreed with this conjecture.^{3,5-8} Recently Ueno, Sun, and Ono³ made a detailed study of the 3D AF Potts models with $Q=3-6$, using the Monte Carlo twist method.^{3,9} They introduced the stiffness exponent ψ to measure a degree of the stiffness of an ordered phase.¹⁰ The stiffness exponents obtained for the IOP's are all not integers with $0 < \psi < D-1$ except for $Q=6$ (which shows no long-range order: $\psi < 0$), which are compared with $\psi=D-1$ (discrete symmetry) and $D-2$ (continuous symmetry) for the ordinary systems with only trivial ground-state degeneracy. These are evidence against the theoretical prediction⁵ that the phase transition is in the universality class of the n ($=Q-1$) vector model. The critical exponents estimated by Ueno, Sun, and Ono indicate that their phase transitions are in new universality classes, as naturally expected when one admits that the IOP's are of a different type. However, Wang, Swendsen, and Kotecký⁷ studied the $Q=3$ model using MC simulations and estimated critical exponent ν for the correlation length that is very close to the value for the 3D XY universality class, in agreement with the theoretical prediction.⁵ Okabe and Kikuchi also obtained a similar result, using large scale MC simulations.¹¹

The $Q=3$ AF Potts model is considered equivalent with the $Q=6$ clock model as in $D=2$ when weak ferromagnetic next-nearest-neighbor couplings are added to the former. Thus Ueno and Mitsubo⁴ studied the latter using the MC twist method. In spite that this model has no nontrivial degeneracy in the ground state, they obtained the corresponding ordered phase at intermediate

TABLE I. Stiffness exponents calculated so far for various models. D_{op} is the dimension of the space, which the order parameter spans, and ‘‘symmetry’’ is that which exists among the possible states in each IOP.

$D = 3$ models (D_{op} , symmetry)	ψ	Kind of IOPS	Ref.
$Q = 3$ AF Potts ($2, Z_6$)	1.20	1	3
Stacked triangular Ising ($2, Z_6$)	1.25	$2, (1)^a$	12
Stacked square frustrated Ising ($2, Z_8$)	1.2	Not examined	13
Ordinary clock ($2, Z_6$)	1.25	1	4
$Q = 4$ AF Potts ($3, O_h$)	1.85	Different	3
$Q = 5$ AF Potts ($4, ?$)	0.7^b	Different	3

^aThe IOP1 is not examined but suggested to exist.

^bPrecision is less than in the others where the errors are about ± 0.05 .

temperatures with stiffness exponent $\psi \simeq 1.2$. This value is in good agreement with the results calculated not only for the $Q = 3$ AF Potts model but also for the stacked triangular AF Ising model¹² and the stacked square frustrated Ising model,¹³ as shown in Table I.

In addition they obtained a distinct twist-angle dependence of ψ of the IOP, which is also evident against the XY character. Since this property had already been obtained in the $Q = 3$ AF Potts model³ (though it was not written there), there exists obvious contradiction between the result obtained by our group and others^{7,11} if one regards their results as an indication of the XY universality class.

In order to study the IOP’s further the GCL model is very useful because it becomes a well-known model such as the ferromagnetic Potts and ordinary clock models, by taking an appropriate set of the energy parameters. Further it can be expected to have the IOP’s in a large temperature region, which can include the noncritical regions, whereas the ordinary one has a narrow IOP region, which prevented a detail study.⁴

As already verified, the twist method has many advantages.^{3,4,14} By means of this method we study the $Q = 6$ GCL model in detail. Further we also study the GCL models of $Q = 4-12$ by the natural iteration method in the pair approximation.¹⁵ We focus on the properties of ordered phases, especially of the IOP’s, though the phase transitions associated with the IOP’s are very interesting. Since determining the nature of transitions needs much more computational efforts than in the present study, we only give preliminary results for it though some are definite and leave a new method for analyzing first-order transitions in a separate paper.¹⁶

The paper is organized as follows. In Sec. II we introduce the general clock models. In Sec. III we review the MC twist method adding new developments. In Sec. IV we present numerical results for the $Q = 6$ model obtained by the MC twist method, explaining the remarkable properties of the IOP’s from various aspect. In Sec. V we give results for several Q ’s calculated in the pair approximation. In Sec. VI we make important remarks and discussions on the IOP’s and their related phase transitions. Summary is given in the last section.

II. THE MODEL

The general Q -state clock model is a generalized version of the Q -state ferromagnetic clock (or Potts) model.

Cardy already studied this model in $D = 2$ and showed a variety of phase transitions,¹⁷ but there is none in $D = 3$ to our knowledge. Its Hamiltonian is given as

$$H = \sum_{\langle ij \rangle} V(\theta_i - \theta_j), \quad (2.1)$$

where the sum is made only over nearest-neighbor (NN) pairs and

$$V(\theta_i - \theta_j) = \sum_{m,n=1}^Q \hat{p}_m(i) \hat{p}_n(j) \varepsilon_{m-n} \quad (2.2)$$

with the spin variable $\{\hat{p}_m(i)\}$ representing the occupation of the m th state at the i th spin

$$\hat{p}_m(i) = \delta(\theta_i - 2\pi m/Q). \quad (2.3)$$

with $m = 1-Q$. Here $\{\varepsilon_m\}$ are the energy parameters with $\varepsilon_m = \varepsilon_{-m} = \varepsilon_{m+sQ}$ for arbitrary integer s , and we set the units of energies as

$$\varepsilon_0 = 0, \quad \varepsilon_{Q/2} = 1 \quad (Q \text{ even}) \quad \text{or} \quad \varepsilon_{(Q-1)/2} = 1 \quad (Q \text{ odd}). \quad (2.4)$$

There remain $[Q/2] - 1$ energy parameters to vary. Figure 1 illustrates these parameters for $Q = 4, 5$, and 6 . Since high degrees of degeneracy are necessary for the IOP’s to occur at least one parameter is required. Thus, the $Q = 3$ model has no IOP. Free energy is given as $F_L(T) = -T \ln Z_L(T)$, where $Z_L = \text{Tr} \exp(-H_L/T)$ in units of $k_B = 1$.

For later convenience, we introduce the uniform, macroscopic spin variable p_n and its Fourier-transform \bar{p}_k in angle:

$$p_n = \frac{1}{N} \sum_i \hat{p}_n(i), \quad (2.5)$$

$$\bar{p}_k = \sum_{n=1}^Q p_n \exp \frac{2\pi i n k}{Q},$$

where k can take $0, \pm 1, \dots, [Q/2]$. While $k = 0$ gives only the normalization ($\bar{p}_0 = 1$), only \bar{p}_1 and \bar{p}_{-1} are used as order parameters (in Sec. V), which are valid in the parameter range we treat in the present study. Varying the energy parameters provides various different models as shown in Table II for $Q = 6$. For the energy parameters, we fix $\varepsilon_2 (= 1)$ and vary ε_1 from 0 to 1.0.

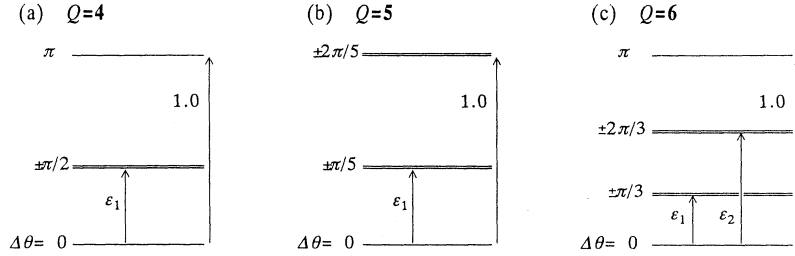


FIG. 1. Energy levels of a neighboring spin pair with relative angles $\Delta\theta$ for the GCL models with $Q=4, 5,$ and 6 in (a), (b), and (c), respectively.

III. THE MONTE CARLO TWIST METHOD

Let us review our twist method adding its new properties restricting to regular systems of classical spins. See Refs. 18 and 19 for the application to random and quantum spin systems, respectively.

One of the ways of giving a twist to the system is to fix rigidly the spins at the opposite boundaries in one direction (α and β) and impose periodic boundary conditions in the other direction(s). These are the boundary conditions (BC's) we use throughout this study. Some work should be done to twist the system, which amounts to the increase in free energy measured from the untwisted state. It depends on how stiff the system is. The method can treat not only the ordered phases that have definite interfaces,²⁰ but also the ones where the interface cannot be defined in spite of nonvanishing stiffness. Therefore, it may be suitable to begin calling this method the twist method instead of the interfacial method and similar ones. Then it may be natural to rename the free-energy difference the *stiffness free energy* for general use instead of the interfacial free energy. The stiffness free energy ΔF is then defined as the difference in the free energy between two systems with and without a twist:

$$\Delta F_L^{\alpha\beta}(T) = F_L^{\alpha\beta}(T) - F_L^{\alpha\alpha}(T) \quad (3.1)$$

for a hypercubic lattice of size L^D except the fixed boundaries. Note $F_L(T) \sim L^D$.

The stiffness free energy defined with the above BC's is assumed to consist of only the singular part, which has been justified in all the calculations made so far for various models (see Refs. 3, 4, 12–14, and 18). Then one can apply finite-size scaling theory²¹ to it at and around the critical temperature T_c :

TABLE II. Energy parameters of the $Q=6$ GCL model that give various known models.

ϵ_1	ϵ_2	Models
1	1	Ferromagnetic $Q=6$ Potts
0.25	0.75	Ferromagnetic $Q=6$ Ising
λ	$0.5 + \lambda$	AF $Q=3$ Potts ^a
$\lambda/(1+9\lambda)$	$(1+6\lambda)/(1+9\lambda)$	Stacked triangular AF Ising ^a

^aThey are obtained through calculating the interface energy at $T=0$ of the systems where ferromagnetic next-nearest-neighbor interactions λ are added.

$$\Delta F_L^{\alpha\beta}(T) = f_{\alpha\beta}(tL^{1/\nu}), \quad (3.2)$$

where $t = (T - T_c)/T_c$ and $f(x)$ is a scaling function that is analytic with respect to x for $L < \infty$; ν is the exponent of the correlation length ξ . This one-parameter scaling form has been confirmed in the MC studies referred to immediately above, and further it can be justified by the following considerations.¹⁹ Thermal fluctuations are $O(T) \sim L^0$ in energy. This is to be compared with when one determines whether a long-range order (LRO) exists or not against thermal fluctuations. Accordingly it is certain that a LRO exists if $\Delta F_L \rightarrow \infty$ for $L \rightarrow \infty$ but it is completely broken if $\Delta F_L \rightarrow 0$ for $L \rightarrow \infty$, assuming that ΔF_L is only the singular part. Since the critical state is neither in a LRO nor disordered, it is unique that ΔF_L at T_c is positive and finite at T_c for $L \rightarrow \infty$. Further ΔF_L at T_c should be proportional to T_c because the opposite forces for ordering and destroying are balanced at T_c . This suggests $\Delta F(T_c)/T_c$ is universal.²² Since the above considerations do not rely on any special models, this form is valid for any classical system that undergoes a second-order phase transition to a disordered phase, under thermal fluctuations. There is another type of phase transitions between an ordered phase with strong rigidity and one with soft rigidity in the systems we are concerned of. One has to apply another scaling form for them as will be given later.

The stiffness exponent is defined by assuming the following asymptotic behavior of ΔF in $L \rightarrow \infty$.

$$\Delta F_L^{\alpha\beta}(T) \sim A_{\alpha\beta} L^{\psi_{\alpha\beta}(T)}. \quad (3.3)$$

As seen from the above discussions, $\psi_{\alpha\beta}$ is negative in the disordered phase. Positive $\psi_{\alpha\beta}(T)$ represents a measure of stiffness of the ordered phase with which the boundary states α and β are compatible. It is an effective value for finite systems because it depends on T in the critical region owing to the finite-size effects. For $L \rightarrow \infty$, $\psi_{\alpha\beta}(T)$ is expected to become a constant $\psi_0 (> 0)$ at all the temperatures where the LRO exists. It is independent of α and β so far as the two boundary conditions $\alpha\beta$ and $\alpha\alpha$ yield an effective difference in the twist.²³ $\psi_{\alpha\beta}(T)$ vanishes at T_c (and also in the region of a quasi-LRO with $\xi = \infty$ if possible). Since $\psi_{\alpha\beta}(T)$ drops sharp in the critical region except for the quasi-LRO, T_c is determined easily and accurately. Since the BC's are fixed one can expect that the estimate of T_c is always an upper limit when the accuracy is sufficient, as confirmed in a $D=2$ Ising model.¹⁴ One can also estimate universal finite-size critical amplitude

$\Delta F(T_c)/T_c$ and critical exponent ν using finite-size scaling (3.2).¹⁴

Since stiffness is a reflection of thermal fluctuations, the stiffness exponent should depend on the type of them. One is familiar to the two types of domain wall and spin wave. Most of those systems with such thermal fluctuations have the ground state that is trivially degenerate. Then the LRO is dominated by only one spin-state or generally a commensurable Fourier component at one of the total energy minima. Thus it may be appropriate to call the ordered phases subject to these types of fluctuations the complete ordered phases (COP), compared with the IOP's. In addition to these types, we argue that there is a novel type of fluctuations proper to the IOP's, as explained in Sec. IV. The stiffness exponent classifies them according to its value as

$$\psi_0 = \begin{cases} D-1 & \text{for domain-wall type} \\ D-2 & \text{for spin-wave type} \\ \text{noninteger} & \text{for a new type.} \end{cases} \quad (3.4)$$

There is a very weak L dependence of $\psi_{\alpha\beta}(T)$.⁴ To take it into account, we introduce a differential definition of the stiffness exponent $\psi_L(T)$, from which we get finite-size scaling for it:

$$\psi_L(T) = \frac{\partial \ln \Delta F_L(T)}{\partial \ln L} = \hat{\psi}(tL^{1/\nu}). \quad (3.5)$$

Then it follows

$$\frac{\partial \psi}{\partial L} \bigg/ \left| \frac{\partial \psi}{\partial T} \right| = \frac{|t|}{\nu L}. \quad (3.6)$$

This proves to have little influence on the estimation of T_c , ν , and $\Delta F(T_c)/T_c$ as long as the sizes extend in a moderate range.¹⁴ For $L > \xi$ below T_c , $\psi_L(T)$ is equal to ψ_0 . Thus one can know the region of $L < \xi$, where $\psi_L(T) < \psi_0$, that is, the region where finite-size effects are large. Further the T dependence of stiffness amplitude A in (3.3) enables one to know the critical region where $\xi \gg 1$.

Now it is appropriate to give a finite-size scaling form for a phase transition from a COP with stiffness exponent $D-1$ to an IOP with $\psi_0 (< D-1)$. Then we have

$$\Delta F_L(T) = L^{\psi_0} g(tL^{1/\nu}), \quad (3.7)$$

where T_c and ν are the quantities relevant to this transition. Here scaling function $g(x)$ behaves asymptotically as

$$g(x) \sim \begin{cases} x^{\nu(D-1-\psi_0)}, & |x| \gg 1 (T < T_c) \\ \text{const}[O(x^0)], & |x| \gg 1 (T > T_c) \\ g_0 + g_1 x, & |x| \ll 1, \end{cases} \quad (3.8)$$

which is different from $f(x)$ in (3.2). Then we get finite size scaling for the stiffness exponent at this transition,

$$\psi_L(T) = \psi_0 + \hat{\psi}(tL^{1/\nu}). \quad (3.9)$$

From (3.9) T_c is determined by the lowest temperature

that satisfies $\psi_L(T_c) = \psi_0$. However, the estimate of ψ_0 (IOP) is usually less accurate, thus yielding large errors in estimating T_c . Let us express $\alpha\beta$ dependence of $\psi_{\alpha\beta}(T)$ in (3.3) as $\psi(T; \phi)$ in terms of twist angle ϕ . Different ϕ 's generally cause different finite-size effects: $\psi_L(T; \phi_1) \neq \psi_L(T; \phi_2)$ for $\phi_1 \neq \phi_2$ except at T_c . Thus we determine T_c by finding a cross point:

$$\psi_L(T_c; \phi_1) = \psi_L(T_c; \phi_2), \quad \phi_1 \neq \phi_2. \quad (3.10)$$

This is valid also for the usual case of (3.2) and will give a better T_c than the previous one as far as the accuracy is enough, though the difference is considered very small.

In the above we have tacitly assumed the case of second-order transitions. In the case of first-order transitions we have found that analyzing ΔE is much more effective than doing ΔF .¹⁶

Let us explain how to calculate the stiffness free energy by Monte Carlo simulation. We first calculate the energies of two systems with and without a twist by the standard method of the MC simulation.²⁴ By making use of $\Delta F_L(T_0) \approx 0$ at T_0 a little above T_c which satisfies $\xi \ll L$, one gets

$$\Delta S(T) = \Delta S(T_0) - \int_{\Delta E(T)}^{\Delta E(T_0)} \frac{1}{T} d(\Delta E(T)). \quad (3.11)$$

This short interval of integration not only reduces the time and errors of calculation, but also enables us to treat highly degenerate systems whose residual entropy is difficult to calculate.

Further there is a great advantage that the errors $\delta\Delta F$ of ΔF are much reduced from $\delta\Delta E$ of ΔE . When one prepares a series of $\Delta E_L(T_i)$ with $i=0, 1, \dots, n(T)$ and interval $\Delta T = (T_0 - T)/n(T)$, where $T_n = T (< T_0)$,

$$\begin{aligned} |\delta\Delta F(T)| &< \frac{\Delta T}{T} \left| \sum_{i=1}^n \delta\Delta E(T_i) \right| \\ &\simeq \frac{T_0 - T}{T} \frac{1}{\sqrt{n(T)}} |\overline{\delta\Delta E}| \end{aligned} \quad (3.12)$$

where $|\overline{\delta\Delta E}| = (1/n) \sum_{i=1}^n |\delta\Delta E(T_i)|$. The reduction was $\frac{1}{10} - \frac{1}{40}$ for the 2D Ising model for $L=50$ with $n=20-40$ (see Ref. 14). This reduction is unchanged when one calculates ΔF from the direct integration of ΔE .

IV. RESULTS OF THE $Q=6$ GCL MODEL BY THE MC TWIST METHOD

To obtain a phase diagram of the model for $\epsilon_1=0 \sim 1$ with $\epsilon_2=1$, calculations are done for the systems of $L=8, 10$, and 12 with about 4×10^4 MC steps per spin, while $T_0=1.75$ ($\geq 1.2T_c$) is set for the starting temperature of the MC simulations. $L=20$ is used for the profiles of some twisted states.

A. Phase diagram

The phase diagram of T versus ϵ_1 is shown in Fig. 2. There are two kinds of IOP's on the smaller side of ϵ_1 . They have four phase boundaries including the one with the disordered phase (DP) and the COP: DP-IOP2 with

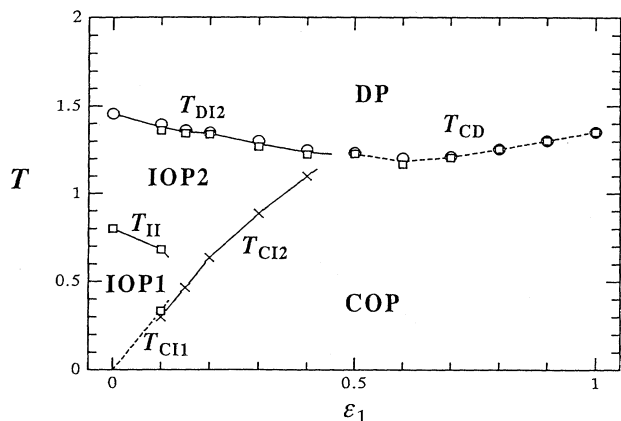


FIG. 2. Phase diagram (temperature vs ε_1) of the $Q=6$ GCL model for $\varepsilon_2=1.0$, obtained by the MC twist method. Solid and broken curves indicate the second and first-order transitions, respectively. Critical points are estimated from the data with twist angles, $\pi/3$ (\square) and π (\circ) and those with both angles (\times). See the text for the detail and the abbreviations in the figure.

critical temperature T_{DI2} , IOP1-IOP2 with T_{II} , COP-IOP1 with T_{CI1} and COP-IOP2 with T_{CI2} . Small ε_1 and moderate temperature are favorable to the IOP's. This property suggests a large contribution of entropy to the existence of these phases, as already pointed out in the previous studies.^{3,4}

According to the analysis of the size dependence of $\Delta E_L(T)$,¹⁵ a coexisting curve of the DP and COP with T_{CD} extends from the ferromagnetic Potts point ($\varepsilon_1=1$) and reaches to $\varepsilon_1=0.5$. There also exists a first-order transition at $\varepsilon_1=0.1$ along the COP-IOP1 boundary. The IOP2-DP transition is continuous though it is less evident. Both the IOP1-IOP2 and IOP2-COP transitions look continuous but there exists the other possibility, since less accuracy and the transitions from a LRO to another one make the analysis difficult. Further discussions will be given in Sec. VI C.

The IOP1 is considered to arise when thermal fluctuations are strong enough to get over the lowest-energy barrier of ε_1 , but much less than the highest. This should hold true also for the IOP2. Then this indicates that T_{CI1} and T_{CI2} are proportional to ε_1 and independent of Q , which is in good agreement with Fig. 2 and the results by the pair approximation in Sec. V (see Fig. 12).

As one will see later there are large entropy contributions to the IOP's. Then it is of considerable interest to observe that the phase diagram qualitatively indicates the following. The entropy is consumed largely and continuously in the large temperature range of the IOP's on the small ε_1 side, then it gets more concentrated as ε_1 becomes large and finally it bursts out as latent heat at the first-order transition at $\varepsilon_1 \geq 0.5$.

B. Two kinds of IOP's

The two kinds of IOP's can be distinguished by the ϕ dependence of $\Delta F_L(T; \phi)$. Let us limit the discussions to

$\varepsilon_1=0.1$ for the time being. Figures 3(a) and 3(b) show the T dependence of ΔF_L , respectively, for weak and strong twists ($\phi=\pi/3, \pi$). In the IOP region ΔF exhibits a noticeable mound which indicates $\Delta S < 0$ in an appreciable part. There is obviously a qualitative difference in the size dependence between ΔF_L 's for both twists. These features are clearly seen in the stiffness exponent $\psi(T)$ in Fig. 4. For $\phi=\pi/3$, $\psi(T)$ crosses with the T axis at three temperatures, 1.42, 0.62, 0.34, which correspond to T_{DI2}, T_{II}, T_{CI1} , respectively, while $\psi(T)$ for $\phi=\pi$ does only at 1.41 corresponding to T_{DI2} . Both $\psi(T)$'s cross at 1.37 and 0.30. In view of the errors we take $T_{DI2}=1.41 \pm 0.01$, $T_{II}=0.62 \pm 0.05$, and $T_{CI1}=0.30 \pm 0.01$ as the best estimates.

For $T_{CI1} < T < T_{II}$, $\psi < 0$ for $\phi=\pi/3$ and $\psi \approx 1.13$ for $\phi=\pi$. These are characteristics of the IOP1 and clear evidence against the XY-like characters, in agreement with the previous results.⁴ On the other hand at $T_{II} < T < T_{DI2}$ ψ are positive but much less than two for both twists, which corresponds to the IOP2. There is some difference between both values of $\psi(T)$ because the accuracy in ΔF is much worse in $\phi=\pi/3$ than in $\phi=\pi$. In the thermodynamic limit we believe both agree and become constant. Then only the $\phi=\pi$ case is reliable for

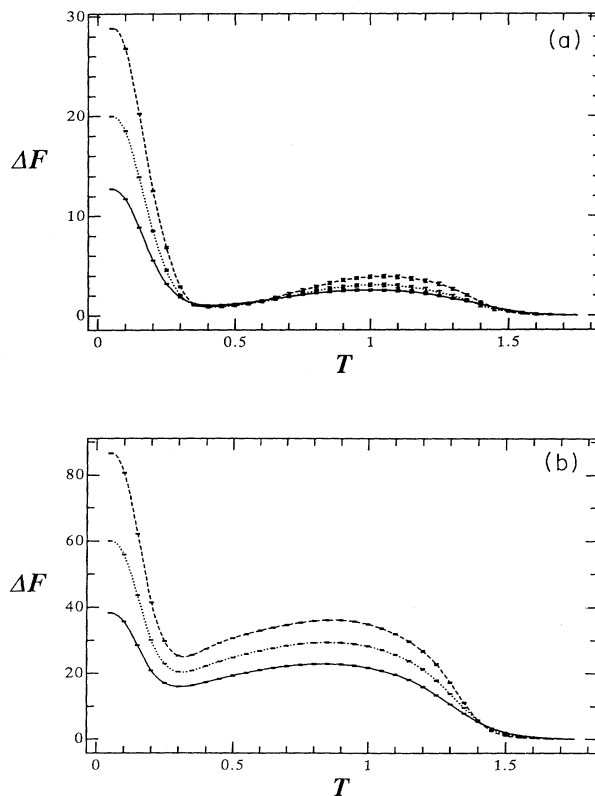


FIG. 3. T dependence of $\Delta F_L(T)$ with $L=8, 10, 12$ at $\varepsilon_1=0.1$ and $\varepsilon_2=1$ of the $Q=6$ GCL model, calculated by the MC twist method with twist angles $\pi/3$ in (a) and π in (b). The splined curves (for guides to the eye) with solid, dotted, and broken lines correspond to $L=8, 10, 12$, respectively. Errors are shown by bars.

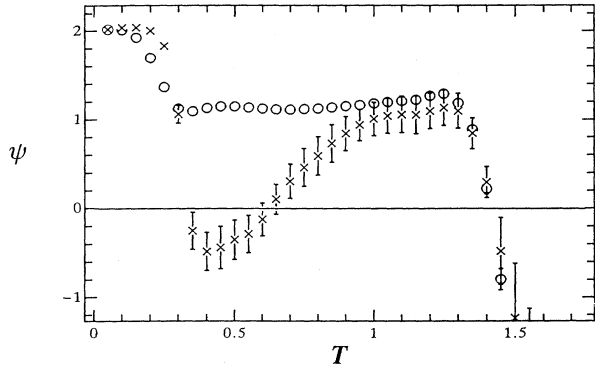


FIG. 4. T dependence of the stiffness exponent of the $Q=6$ GCL model at $\varepsilon_1=0.1$ and $\varepsilon_2=1.0$ for two twist angles, $\phi=\pi/3$ (\times) and π (\circ), calculated by the MC twist method. Errors are shown by bars though those smaller than the symbols are not given.

both IOP's, where ψ varies from 1.1 to 1.3 outside the critical region. Since there is no finite-size effect there as explained in Sec. III, ψ_0 must be a constant around 1.2. This value is in good agreement with those of the models previously studied (see Table I).

From the ϕ dependence of $\psi(T)$ in the IOP1 one sees that the system is disordered between the two dominating states, though being critical might be right rather than being disordered as will be discussed in Sec. VI B. Then the one-spin distribution function of the IOP1 becomes as in Fig. 5(b), in contrast with that of the COP in Fig. 5(d).

In the IOP2 stiffness exists for any twist and the order is as soft as the IOP1. The order is a little more stiff than that in the XY -like ordered phase. From examining profiles of the twist states and a spin configuration as shown later, we obtain the one-spin distribution function for this phase as Fig. 5(c). In Fig. 6 we show the T dependence of ψ at $\varepsilon_1=0.3$ and 0.5. For $\varepsilon_1=0.3$, we obtain $T_{DI2} \simeq 1.30$ and $T_{CI2} \simeq 0.90$ in the similar way to the case of $\varepsilon_1=0.1$. Between these critical points, ψ is positive but much smaller than two for both twists. Since critical fluctuations are large and dominant for $\phi=\pi/3$ in this narrow region, ψ cannot reach to ψ_0 . For $\phi=\pi$ there is a narrow terrace with $\psi \simeq 1.1$, which is close to $\psi_0 \simeq 1.2$ for $\varepsilon_1=0.1$. For $\varepsilon_1=0.5$, since any terracelike behavior is not seen, we consider there is only one transition at $T_{CD} \simeq 1.26$ to the COP. For $\varepsilon_1 > 0.5$, the obtained results (which are omitted) obviously show only one transition to the COP.

C. Profiles and spin configurations of the IOP's

In order to understand the IOP's it is very useful to look at their profiles and spin configurations in the twisted states. We have calculated profiles of systems with $\varepsilon_1=0.1$ of size $L=20$ for a few twists. They represent a distribution of each clock state averaged within each cross section perpendicular to the twist axis, thus as a function of the coordinate of cross section. We show two kinds of profiles below: one is taken at one time and the

other is averaged over 1000 MC steps per spin. Since the center-of-mass of the profiles change in time, the former is useful to see patterns of distributions, and, in spite of being instant, it has an average property done over a large number of the spins on a cross section.

Let us start with the IOP1. Figures 7(a) and 7(b) show the snapped profiles at $T=0.55$ for $\phi=0$ and $\pi/3$, respectively. They have the common features: there exist mixed states consisting of two adjacent states in the inner part. Although the spin states are different on the boundary sides due to different boundary conditions, this difference makes almost no difference in energy, thus in free energy (see Fig. 16 given later). This is consistent with the result obtained above that there is no stiffness

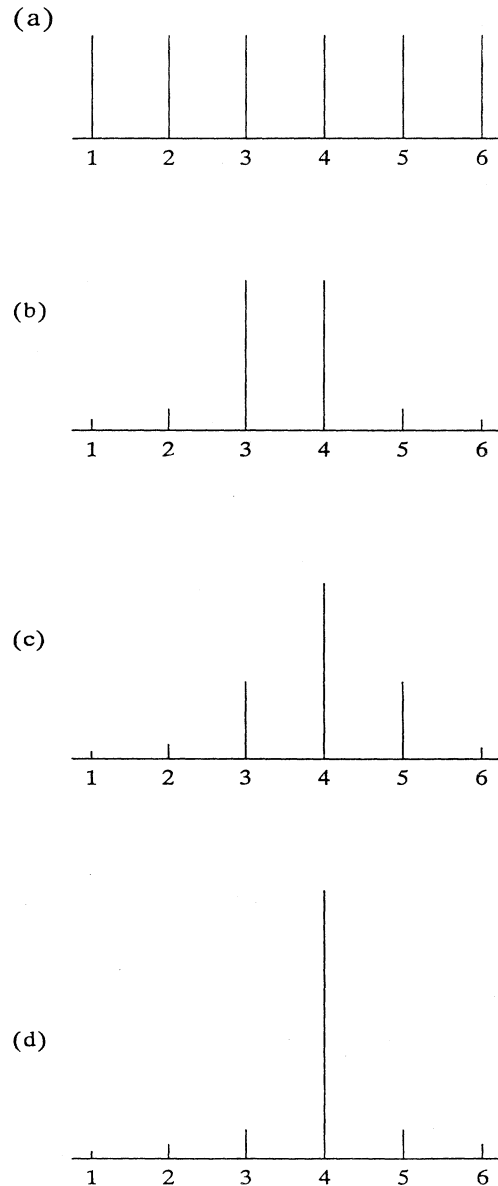


FIG. 5. Schematic one-spin distribution functions (probability vs clock-state) of the $Q=6$ GCL model for the DP in (a), the IOP1 in (b), the IOP2 in (c) and the COP in (d).

for $\phi = \pi/3$. However, in the profiles for stronger twist $\phi = 2\pi/3$ as shown in Fig. 7(c), there are two regions of different IOP1's [\square/\times] and [\times/\circ] and a large intermediate zone separating them. These IOP's are adjacent with each other having a common state (\times). It is noted that the profiles of the other states (\square and \circ) cross sharp in the intermediate zone. Therefore, it is reasonable to consider that this zone works as a buffer so as to prevent spins in states with large angles ($|\Delta\phi| > \pi/3$) from getting close to each other because otherwise it costs large energy. It is the common state that plays the role of a buffer. This suggests that the number of NN pairs in different states by $\phi > \pi/3$ depends on the size much more weakly than in L^2 (see Ref. 4). This size dependence is nothing but the stiffness exponent ($\psi_0 \simeq 1.2$) because NN pairs with $\phi = \pi/3$ do not contribute in the IOP1.

The averaged profiles for the IOP1 are shown in Fig. 8. They are qualitatively the same as the snapped ones. Although the profiles for $\phi = 2\pi/3$ look very smooth in Fig. 8(c), there still remain some characteristics of the IOP1 that are very consistent with the profiles for $\phi = 0$ and $\pi/3$. Probably much larger sizes are needed to present the IOP1 clearly.

Next is the IOP2. Figures 9(a) and 9(b) show, respectively, snapped and averaged profiles for $\phi = 0$ at $T = 1.2$. Both reveal that such a distribution as in Fig. 5(c) is al-

most realized, even locally, though their fluctuations are very large as seen in Fig. 9(a). On the other hand, the profiles for $\phi = \pi/3$ in Figs. 10(a) and 10(b) exhibit one intermediate zone between two regions in different but adjacent states, which are considered IOP2's [$\times/\circ/\square$] and [$\circ/\times/*$]]. In these IOP2's there are two common states (\circ and \times). Thus these play as buffers, as is seen in the figures. It is interesting to observe that these buffer states are the same as the IOP1. Then this suggests that a certain IOP1 exists at the pass in the phase space,

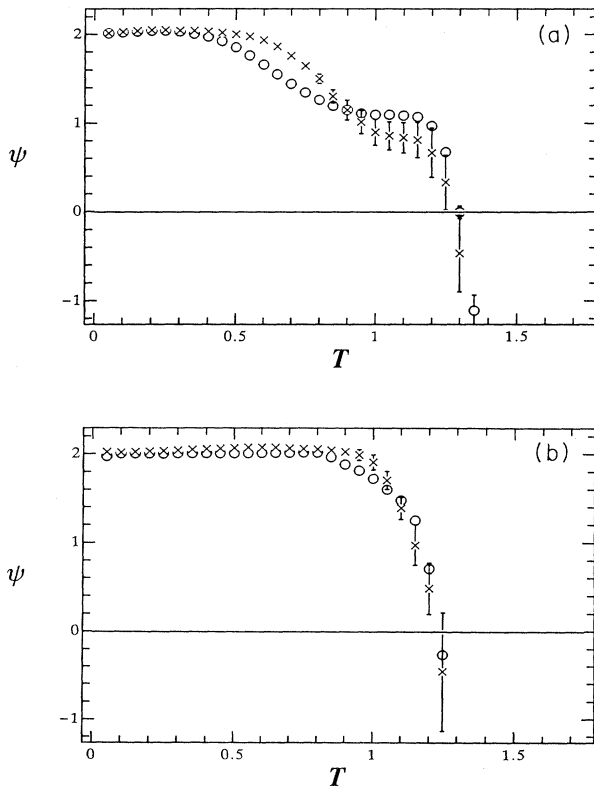


FIG. 6. Stiffness exponents vs temperature of the $Q = 6$ GCL model at $\epsilon_1 = 0.3$ in (a) and 0.5 in (b) for twist angles $\phi = \pi/3$ (\times) and π (\circ), calculated by the MC twist method.

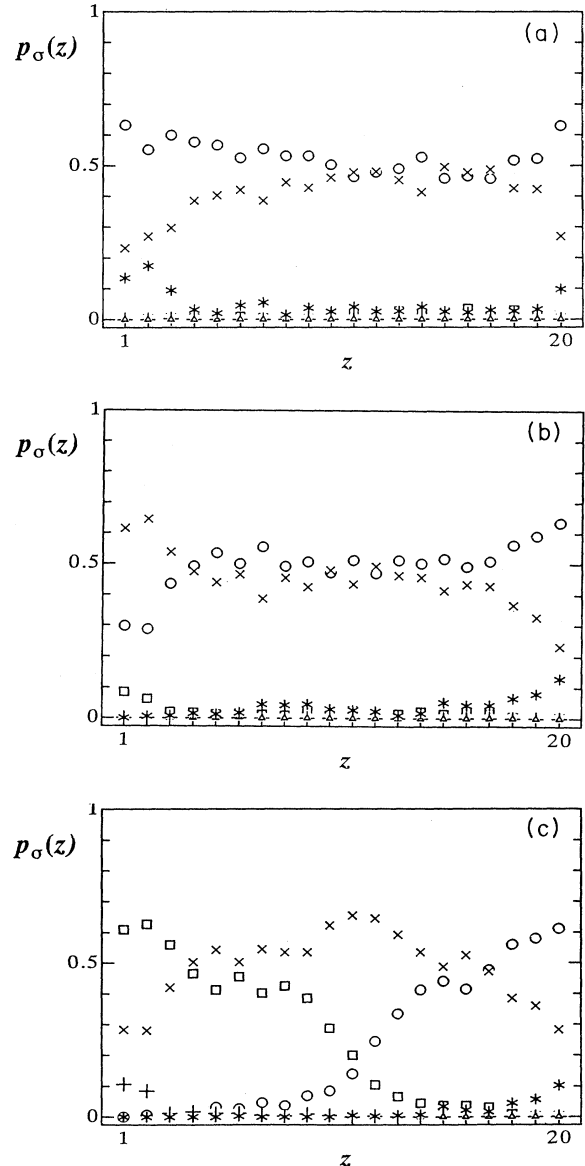


FIG. 7. Snapped profiles of the IOP1 for each spin-state σ at $T = 0.55$ for $\epsilon_1 = 0.1$ of the $Q = 6$ GCL model twisted by $\phi = 0$ in (a), $\pi/3$ in (b), and $2\pi/3$ in (c), obtained by MC simulations. Each state is represented as 1 (\circ), 2 (\times), 3 (\square), 4 ($+$), 5 (\triangle), or 6 ($*$). State 1 is always fixed at the right boundary ($z = 21$), whereas at the left boundary ($z = 0$) states 1, 2, and 3 are fixed, respectively, in (a), (b), and (c).

which connects two adjacent IOP2's and thus the IOP1 is higher in free energy than the IOP2. Similarly, in the IOP1 regime, we can say that a COP is at the pass between two adjacent IOP1's (see Figs. 7 and 8).

In the IOP1 these buffers work well and enclose excited nondominant states in a small space, so that only two adjacent states are dominant. In the IOP2 their work becomes less effective because of strong thermal fluctuations, so that three adjacent states are dominant and the IOP2 appears at higher temperatures above the IOP1. From the above results we can describe thermal fluctua-

tions in the IOP1. Each dominant excitation is a (kind of) domain of an IOP1-state adjacent to the IOP1-state (that bears the LRO) and such a domain is surrounded by a buffer. This type of thermal fluctuations is characterized in a large scale by the nonintegral stiffness exponent. In the IOP2 thermal fluctuations become complicated but we consider they are similar to those in the IOP1.

It is of considerable interest to see spin configurations in the IOP's. Figures 11(a) and 11(b) are cross sections of the IOP1 and IOP2, respectively, from the data for $\phi = \pi/3$ at $\varepsilon_1 = 0.1$. In order to have spin configurations clearly but roughly seen, we have employed the following process, which approximately smears thermal fluctuations of the shortest wavelength without decimation. For each spin we average its phase angle together with those of its NN spins only on the cross section. Note that we use only the original configuration without replacing the averaged values until this process is done for all the spins.

In Fig. 11(a) for the IOP1, two adjacent states (\circ and \times) are almost completely dominant with equal weight, so that they are percolated even on a cross section, which is reminiscent of microemulsion.²⁵ Figure 11(b) for the IOP2 shows that one state (\times) is most dominant. Its adjacent states (\circ and \square) form unpercolated domains on a cross section, but it is not certain whether they remain unpercolated even in the $D = 3$ space or not. Though

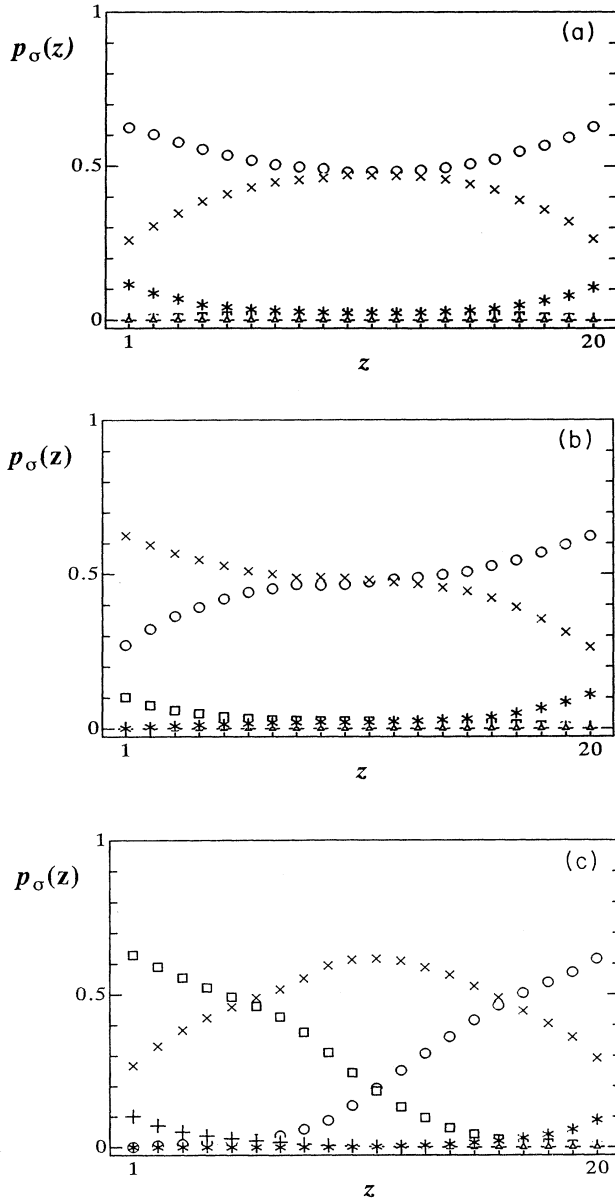


FIG. 8. Averaged profiles of the IOP1 at $T = 0.55$ for $\varepsilon_1 = 0.1$ of the $Q = 6$ GCL model twisted by $\phi = 0$ in (a), $\pi/3$ in (b), and $2\pi/3$ in (c), obtained by MC simulations. Average time is 1000 MC steps per spin. See the caption of Fig. 7 for the notations and boundary conditions.

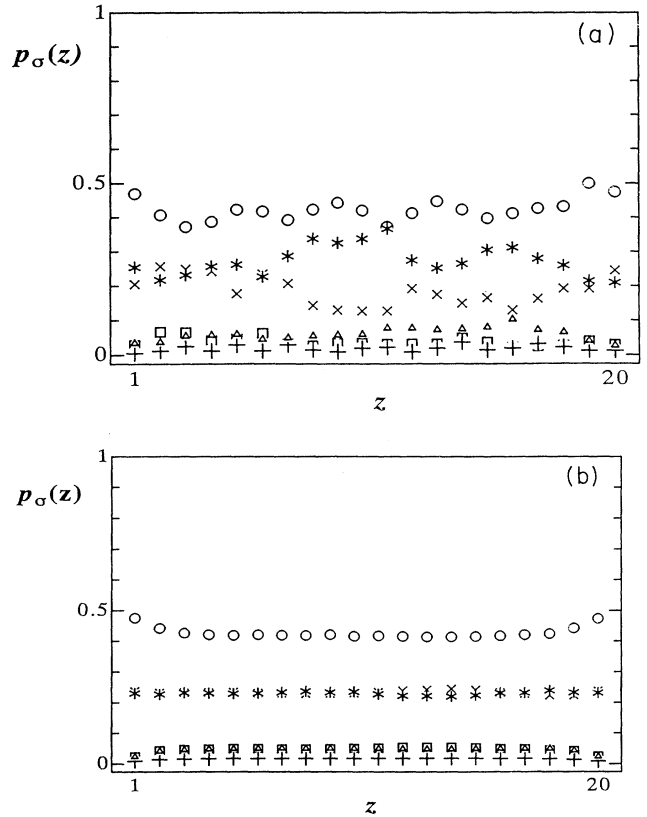


FIG. 9. Snapped (a) and averaged (b) profiles of the IOP2 at $T = 1.2$ for $\varepsilon_1 = 0.1$, $\varepsilon_2 = 1$ of the $Q = 6$ GCL model with untwisted boundary conditions ($\phi = 0$), obtained by MC simulations. See the caption of Fig. 7 for the notations.

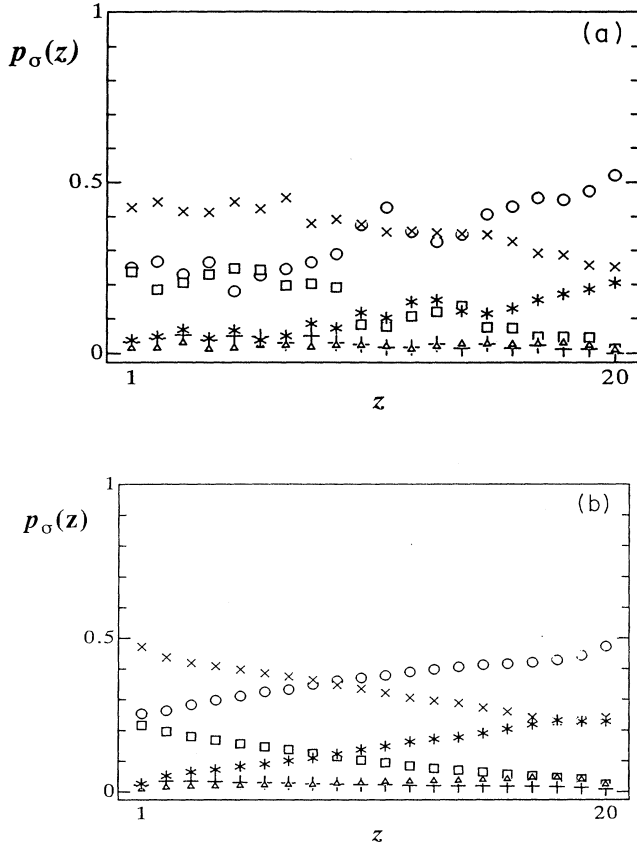


FIG. 10. Snapned (a) and averaged (b) profiles of the IOP2 at $T=1.2$ for $\varepsilon_1=0.1$ and $\varepsilon_2=1$ of the $Q=6$ GCL model twisted by $\phi=\pi/3$, obtained by MC simulations. See the caption of Fig. 7 for the notations.

they are not “physical clusters” but “geometrical clusters,”²⁶ we conjecture that they are percolated through the system, which is probably only the peculiar property that makes the IOP2 differ from the COP. Very recently this has been confirmed.²⁷ Further discussions will be given in Sec. VI B.

V. RESULTS OF Q -STATES GCL MODELS IN THE PAIR APPROXIMATION

As mentioned in Sec. II we cannot define the order parameters, which distinguish between the COP and IOP2. Nevertheless it may be helpful to understand the present problems from such a theoretical point of view as what properties will be obtained by an elementary approximation.

A. Pair approximation by means of the natural iteration method

Since the spin component in the clock models is large in number, there are too many variables in the self-consistent equations to easily solve them even by computers. In such a case the natural iteration method is very

useful.¹⁵ Let x_{mn} be the probability that a pair of spins are in the m th and n th clock states and p_m be the one of finding a spin in the m th state. There are the following restrictions among them:

$$\sum_m \sum_n x_{mn} = 1, \quad p_m = \sum_n x_{mn}, \quad x_{mn} = x_{nm}. \quad (5.1)$$

The energy and entropy per spin in $L \rightarrow \infty$ are given in terms of them.

$$E = \frac{1}{2}z \sum_m \sum_n \varepsilon_{mn} x_{mn} - \sum_m h_m p_m, \quad (5.2)$$

$$S = (z-1) \sum_m K(p_m) - \frac{z}{2} \sum_m \sum_n K(x_{mn}) + \frac{z}{2} - 1, \quad (5.3)$$

where z is the coordination number, h_m the applied field and $K(x) = x(\ln x - 1)$. We treat only the case with no applied field. In order to treat every x_{mn} independently we define the free energy (multiplied by $\beta = T^{-1}$) that includes the constraint term with an unknown parameter λ :

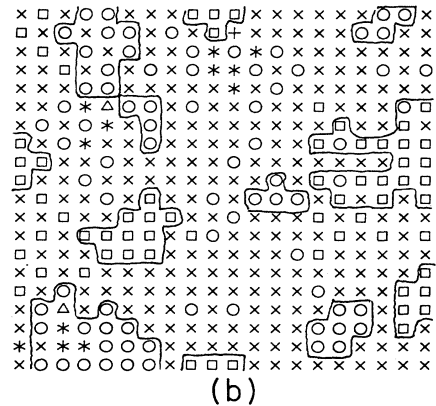
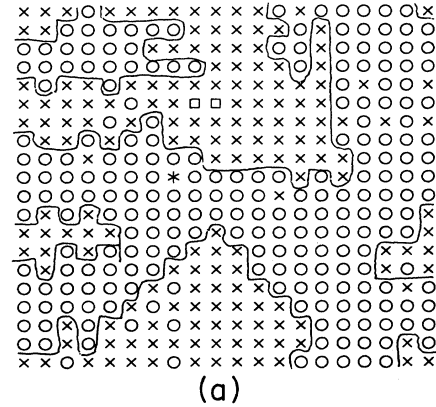


FIG. 11. Spin configurations on a cross section at $T=0.55$ for the IOP1 (a) and at $T=1.2$ for the IOP2 (b) in the $Q=6$ GCL model with $\varepsilon_1=0.1$ and $\varepsilon_2=1$, obtained by MC simulations. The symbols represent the states as 1 (\circ), 2 (\times), 3 (\square), 4 ($+$), 5 (\triangle), and 6 ($*$). They have been obtained after smearing out the shortest-wavelength fluctuations, for the detail of which see the text. The contours are the walls between the regions of the dominating states with barrier energy ε_1 . These configurations are part of the data used in Figs. 7(b) and 9(a).

$$\Phi = \beta E - S + \beta \lambda \left[1 - \sum_m \sum_n x_{mn} \right]. \quad (5.4)$$

Minimizing Φ with respect to every x_{mn} leads to

$$x_{mn} = \exp(2\beta\lambda/z - \beta\varepsilon_{mn})(p_m p_n)^{1-1/z}, \quad (5.5)$$

$$\exp(-2\beta\lambda/z) = \sum_m \sum_n \exp(-\beta\varepsilon_{mn})(p_m p_n)^{1-1/z}, \quad (5.6)$$

and $\lambda = \Phi$. Then using (5.5), (5.6), and (5.1) one can solve these equations in an iterative way by starting an arbitrary state $\{p_m\}$, which has the symmetry of a phase of interest.

Taking $z=6$, we look for the three kinds of solutions corresponding to the DP, IOP1 and COP with precision 10^{-8} for the free energy. With $\varepsilon_2=1.0$ fixed, ε_1 is varied from 0 to 1.0 for the $Q=4,5,6$ models, and ε_1 is taken only at $\varepsilon_1=0.1$ and 1.0 for $Q=8,10,12$.

Using \bar{p}_1 and \bar{p}_{-1} in (2.5) we define the order parameters:

$$\bar{p}_c = \sum_{n=1}^Q p_n \cos \frac{2\pi n}{Q}, \quad (5.7a)$$

$$\bar{p}_s = \sum_{n=1}^Q p_n \sin \frac{2\pi n}{Q}. \quad (5.7b)$$

From the comparison with Fig. 5, \bar{p}_s has the same symmetry as the one-spin distribution function of the IOP1. On the other hand, \bar{p}_c has the same symmetry as both the ones of the COP and IOP2. We have no other order parameters to distinguish them in the pair approximation because \bar{p}_k with $|k| > 1$ is theoretically unacceptable in the parameter range of concerned and also inconsistent with the present MC results in Sec. IV. We do not consider this difficulty solved, even if the cluster approximation is raised to any degree as long as these distributions have the same symmetry. The conjecture on the characteristics of the IOP2 given in Sec. IV suggests a different type of order parameter. To be sure, we note that there is no spatially regularly modulated order in the IOP's within the limit of sizes we took because otherwise one got $\Delta F_L < 0$.

B. The results

Figure 12 shows the phase diagrams for the GCL models with $Q=4,5,6$. The agreement with the MC results for $Q=6$ (Fig. 2) is qualitatively very good if we neglect the deficiency of this method. In particular the upper phase boundary has the same tendency of the ε_1 dependence, including the result that the critical point is larger at $\varepsilon_1=0$ than at $\varepsilon_1=1.0$. At $\varepsilon_1=1$, $T_{CD} \approx 1.350$ agrees well with 1.35 obtained in Sec. IV, which is attributed to the strong discontinuity. In addition, the lower critical point T_{CI} on the small ε_1 side is proportional to ε_1 . However there is a large difference in the nature of the phase transitions provided that our conclusion given in Sec. IV is correct. That is, all the phase boundaries in Fig. 12 are of first order. However the jump in energy is considerably smaller at the boundaries of the IOP; for example, $\Delta E \sim 0.006$ at $T_{DI} \approx 1.54$ and $\Delta E \approx 0.05$ at $T_{CI} \approx 0.30$ when $\varepsilon_1=0.1$. Since the cluster approximations tend to

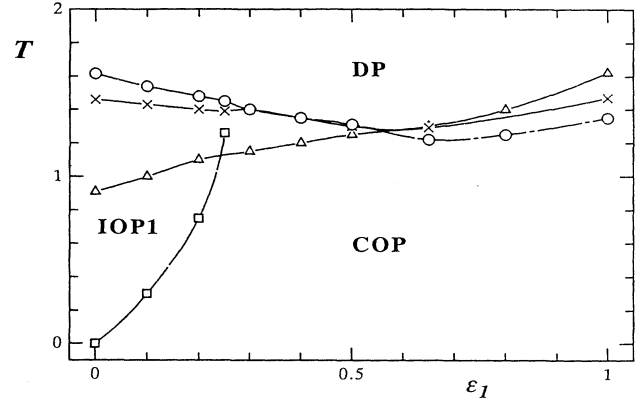


FIG. 12. Phase diagrams (T vs ε_1) of the GCL models for $Q=4$ (Δ), 5 (\times), and 6 (\circ) with $\varepsilon_2=1.0$, calculated in the pair approximation. The boundary (\square) between the IOP1 and COP is unchanged among $Q=4,5,6$ so far long as the IOP continues along the boundary. Splines are the guide to the eye.

err on the first-order side,²⁸ these discontinuities will decrease and, in particular, the former will disappear as the degree of approximation is raised. We had half speculated that the phase boundary between the IOP2 and the COP might disappear in this approximation because both have the same symmetry. As a matter of fact the IOP1 has replaced the IOP2.

Then one might naturally doubt the validity of the results of T_{DI} and thus of comparing them with the MC results. However, we have also obtained that at $T_{CI} < T < T_{DI}$ the difference in free energy between two solutions for \bar{p}_s and \bar{p}_c is not so large; especially it is quite small as T approaches T_{DI} and vanishes at T_{DI} . Therefore near T_{DI} the solution for \bar{p}_c is almost equal to the IOP2 and T_{DI} is also the critical point for the IOP2.

Figure 13 shows the T dependence of the order parameters \bar{p}_c and \bar{p}_s at $\varepsilon_1=0.1$ for $Q=6$. This consists of \bar{p}_c below $T_{CI}=0.30$ and \bar{p}_s at $T_{CI} < T < T_{DI}=1.54$. It

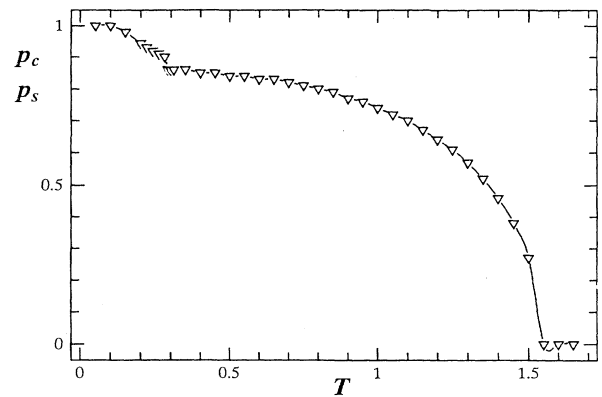


FIG. 13. Temperature dependence of the order parameters of the $Q=6$ GCL model with $\varepsilon_1=0.1$ and $\varepsilon_2=1.0$, calculated in the pair approximation. The curve consists of \bar{p}_c below $T_{CI}=0.30$ and \bar{p}_s for $T_{CI} < T < T_{DI}=1.54$.

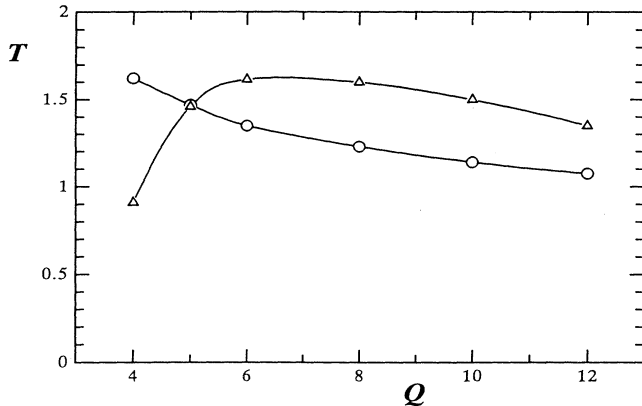


FIG. 14. Critical temperature vs clock-state number at $\epsilon_1=0.0$ (Δ , T_{DI}) and $\epsilon_1=1.0$ (\circ , T_{CD}) of the Q -state GCL model with $\epsilon_2=1$, calculated in the pair approximation.

shows a small discontinuity about 0.037 at T_{CI} . This behavior is quite consistent with the specific heat behavior (which has been omitted).

Concerning the Q dependence of the phase diagrams in Fig. 12, the following are remarkable: (i) For the upper critical temperature, T_{DI} increases with Q on the small ϵ_1 side, whereas T_{CD} decreases against Q on the opposite side. In contrast to it, (ii) the lower critical temperature T_{CI} does not depend on Q . The first (i) is very good material for instruction to explain the difference between the LRO's formed owing to entropy gain and energy gain, details of which is given in Sec. VI. From the second property (ii), it follows that there are only two relevant spin states adjacent to the dominating state that destroy the COP and form the IOP1. This is quite consistent with the one-spin distribution of the IOP1 obtained in Sec. IV.

To investigate further the Q dependence of the upper critical temperature we have calculated the T_c 's only at $\epsilon_1=0$ and 1 for $Q=8, 10, 12$, which are given in Fig. 14. At $\epsilon_1=1$ the decreasing tendency is kept, whereas T_{DI} at $\epsilon_1=0$ makes a maximum at $Q=6$ and decreases with Q increasing. These results are discussed in VI A.

VI. REMARKS AND DISCUSSIONS

A. Ordering due to entropy gain

We first look at the properties of ΔS and ΔE obtained by the MC twist method at $\epsilon_1=0.1$, $\epsilon_2=1.0$ (see Figs. 15 and 16). ΔS is negative at low temperatures that are almost in the IOP1 region and the lower half of the IOP2 region. In these regions, $\Delta S < 0$ is attained with little energy cost; ΔE is even negative for $\phi=\pi/3$, and it is positive and comparable to $T|\Delta S|$ for $\phi=\pi$. Since negative ΔS contributes largely to positive ΔF , this is direct evidence of ordering due to entropy gain. At higher temperatures both ΔS and ΔE become positive, but ΔS is still much smaller than that of the COP.

In the IOP2 region the entropy seems to change its role

and work to destroy the order as the temperature increases. However, the following idea may be reasonable. Roughly speaking, there are two different kinds of configurations in the twisted states: One costs little energy and contributes to keeping the order (reducing ΔS), whereas the other costs much energy and contributes to destroying it (increasing ΔS). At higher temperatures the latter becomes predominant. Thus it results in $\Delta S > 0$ in total, but ΔS is still much lower in the IOP's than in the COP as seen in the figure in spite of temperature being much larger. It is noted that the IOP2 is protected from becoming disordered by the second barrier ϵ_2 .

Next we discuss the Q dependence of the critical points obtained in the pair approximation (see Fig. 14). At $\epsilon_1=1.0T_{CD}$ decreases monotonously against increasing Q . In the ferromagnetic Potts models with large Q the energy almost dominates below T_{CD} , whereas the entropy does above T_{CD} , as is also understood from the mean-field results.²⁹ Thus as Q increases only the entropy contribution becomes large, reducing T_c . On the other hand, at $\epsilon_1=0.0$ there is a maximum T_{DI} for $Q=6$. The first increase is clear evidence that the entropy contributes to the IOP because the increase of the degrees of freedom leads to large entropy. However, its most frequent effect for the IOP is limited to some extent. Further increase of them may merely contribute to the complete disorder. This tendency is very similar to the T dependence of ΔS explained above. This similarity is reasonable because

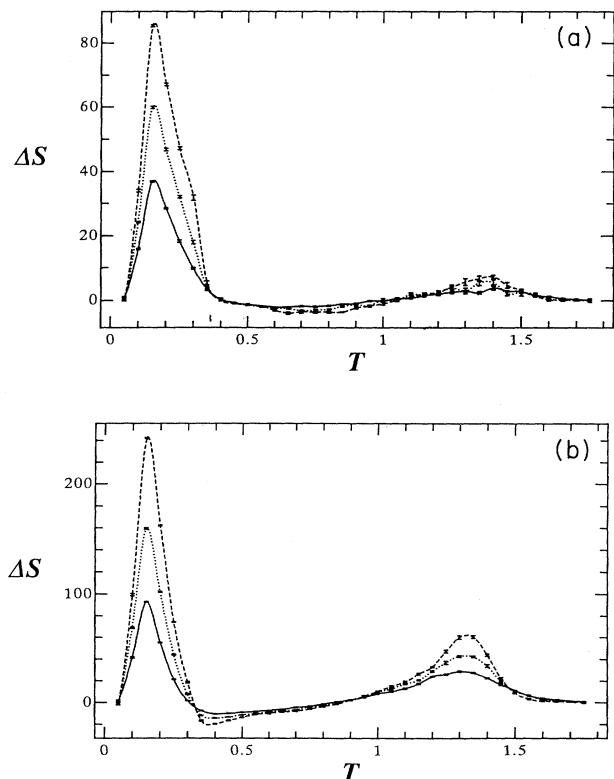


FIG. 15. Excess entropy vs temperature at $\epsilon_1=0.1$ and $\epsilon_2=1$ of the $Q=6$ GCL model twisted by $\pi/3$ in (a) and π in (b), calculated by the MC twist method.

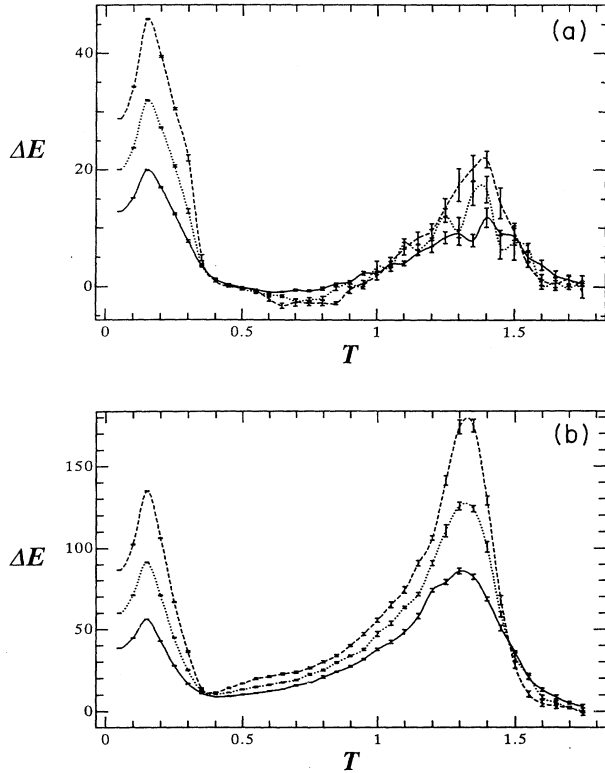


FIG. 16. Excess energy vs temperature at $\varepsilon_1=0.1$ and $\varepsilon_2=1$ of the $Q=6$ GCL model twisted by $\pi/3$ in (a) and π in (b), calculated by the MC twist method.

both larger Q and T have the effect of increasing the degrees of available freedom to get over the energy barrier of ε_2 .

It is worth stressing that the following is remarkable: T_c is higher at small ε_1 than at large ε_1 in a fairly large region of Q in spite of noncompeting interactions being reduced. This kind of property has never been found to our knowledge in the highly degenerate systems brought about by competing interactions.³⁰ Thus one may say that the highly degenerate models without competing interactions can make best use of entropy for ordering.

B. Nature of the IOP's

In the profiles of the IOP1 for $\phi=2\pi/3$ [see Figs. 7(c) and 8(c)], the two dominant states that are not common to the two adjacent IOP's cross sharply. This reveals the following important property of the IOP1. The two dominant states in an IOP are well mixed because otherwise two uncommon states in the twisted state can get in the neighborhood with a low probability, thus resulting in a dull crossing or large probability of coexistence in a cross section. Further mixing well yields extremely large entropy, which is quite consistent with the above conclusion.

We have defined the IOP's as the soft phases with a nonintegral stiffness exponent. Being noninteger suggests a manifestation of the *fractal* feature of the IOP's such

that the number of NN pairs with relative angle $2\pi/3$ increases in power of L with a fractional number, when the twisted state is compared with the untwisted state. Twisted states are considered to be condensed states of the largest-wavelength excitation in the finite untwisted system. Therefore, this fractal feature is inherent in the IOP's irrespect of the BC's. Then it follows that the majority states of the IOP's are not disordered with each other, but they are critically coexisting. This description is consistent with the results obtained from the geometrical description formulated recently.³¹

The IOP1 has already been obtained both in the 3D ordinary $Q=6$ clock model,⁴ and the 3D $Q=3$ AF Potts model,³ while an IOP2 was found for the first time in the 3D stacked triangular AF Ising model,¹² though their differences were not clearly noticed before. Further it should be noted that the estimates of the stiffness exponents in various models in Table I suggest the existence of the following universality. They are classified according to the dimensions of the space in which the order parameter spans, D_{OP} : $\psi_0 \approx 1.2, 1.8, 0.7$ for $D_{OP}=2, 3, 4$, respectively.

C. Nature of the phase transitions of the IOP's

We have argued that the IOP's are a different type of ordered phase. Then it is natural to expect the same thing also for the phase transitions related to the IOP's. The MC results suggest second-order transitions along some phase boundaries of the IOP's. It is of interest to consider this problem from the symmetric point of view. As one immediately sees from the comparison of the one-spin distributions in Fig. 5, there is no symmetry change at the COP-IOP2 transition, so far as the uniform macroscopic symmetry is concerned. Since there is little possibility of being a modulated order, this is a transition without symmetry breaking. Though the nature of the transition is not evident, being second order is favorable because, since the first-order transition has no restriction of symmetry, no symmetry change is least probable. If this conclusion is true, then this transition is well explained as being topological in terms of the percolation of wall bonds, which represent physical connection between clusters in adjacent states, according to the geometrical formulation.³¹

On the other hand, at the IOP1-COP and IOP1-IOP2 transitions the symmetries of both phases concerned are not in the relation of group and subgroup. Since this heterogeneous symmetry change is against the Landau theory for the second-order transition but reasonable at the first order,³² both transitions are considered discontinuous.

VII. SUMMARY

The present study has investigated an energy-parameter line of the $Q=6$ GCL model that does not include the ordinary clock model. However, we do have the interesting results and insight into the IOP's and the LRO due to entropy gain, which are quite consistent with the results previously obtained for various models. The following are the results of the $Q=6$ GCL model with

$\varepsilon_2 = 1.0$ obtained by the MC twist method. (i) The phase diagram with $0 < \varepsilon_1 < 1$ has a variety of ε_1 dependence, including two kinds of the IOP's on the small ε_1 side and the coexisting line extending to the Potts point $\varepsilon_1 = 1$. (ii) Both IOP's have $\psi \approx 1.2$ except that the IOP1 exhibits $\psi < 0$ only for a weakest twist ($\psi = \pi/3$). Two adjacent spin states dominate the IOP1, whereas three adjacent states do the IOP2, which exists above the IOP1 or the COP. (iii) Thermal fluctuations in the IOP's are characterized by their patterns, which are of soft structures with buffers that prevent spins in different states by $\phi > \pi/3$ from getting direct contact. (iv) The DP-COP and IOP1-COP transitions are discontinuous. The IOP2-COP is suggested to be continuous, whereas the IOP1-COP and IOP1-IOP2 transitions are not evident. (v) The IOP2-COP transition breaks no uniform macroscopic symmetry, and is strongly suggested to be of a different type.

The following are the results obtained in the pair approximation. (i) The phase diagram obtained for $Q = 6$ is qualitatively in good agreement with the one obtained by the MC study, though the IOP2 could not be obtained and all the transitions are of first order. (ii) For $Q = 4, 5, 6$, the lower transition points T_{CI} is independent of Q and proportional to ε_1 . T_{DI} at $\varepsilon_1 = 0$ exhibits unex-

pected Q dependence, in contrast to the monotonous decreasing of T_{CD} at $\varepsilon_1 = 1$ with increasing Q .

We hope these many interesting results and suggestions to be examined and investigated further.

Note added in proof. In the 2D GCL model with next-nearest-neighbor interactions the IOP2 has been found by H. Shioda and Y. Ueno [J. Phys. Soc. Jpn. (to be published)].

ACKNOWLEDGMENTS

The authors would like to thank K. Ishida, P. Nightingale, I. Ono, Y. Ozeki, T. Satomura, H. Shioda, R. H. Swendsen, and A. Yamagata for discussions. This work was partly supported by Grant-in-Aid for Scientific Research on Priority Areas, Computational Physics as a New Frontier in Condensed Matter Research, from the Ministry of Education, Science and Culture. This work was carried out under the ISM Cooperative Research Program (93-ISM.CRP-44). The numerical calculations were performed on the supercomputers in Institute for Molecular Science of Okazaki National Research Institutes, Institute of Statistical Mathematics, Computer Center of Hokkaido University and Computer Center of the University of Tokyo.

¹F. Y. Wu, J. Appl. Phys. **55**, 2421 (1984).

²A. N. Berker and L. P. Kadanoff, J. Phys. A **13**, L259 (1980).

³Y. Ueno, G. Sun, and I. Ono, J. Phys. Soc. Jpn. **58**, 1162 (1989); **61**, 4672(E) (1992).

⁴Y. Ueno and K. Mitsuho, Phys. Rev. **43**, 8654 (1991). Note the hexagonal lattice was used there.

⁵J. Banavar, G. S. Grest, and D. Jasnow, Phys. Rev. B **25**, 4639 (1982); Phys. Rev. Lett. **45**, 1424 (1980).

⁶I. Ono, Prog. Theor. Phys. Suppl. **87**, 102 (1986).

⁷J.-S. Wang, R. H. Swendsen, and R. Kotecký, Phys. Rev. **42**, 2465 (1990).

⁸Ono's result for the $Q = 3$ model is exceptional though it was later corrected (see Refs. 3 and 7).

⁹The development was initiated by G. Sun, Y. Ueno, and Y. Ozeki, J. Phys. Soc. Jpn. **57**, 160 (1988).

¹⁰The stiffness exponent is defined in Sec. III. We shall use a Greek letter (ψ) hereafter instead of a , as used before.

¹¹Y. Okabe and M. Kikuchi (private communication).

¹²K. Mitsuho, G. Sun, and Y. Ueno, in *Cooperative Dynamics in Complex Systems*, edited by H. Takayama (Springer, Berlin, 1989), p. 49.

¹³G. Sun and Y. Ueno, Z. Phys. **82**, 425 (1991).

¹⁴H. Shioda and Y. Ueno, J. Phys. Soc. Jpn. **62**, 970 (1993); H. Shioda, Master's thesis, Tokyo Institute of Technology, 1993.

¹⁵R. Kikuchi, J. Chem. Phys. **60**, 1071 (1974).

¹⁶Y. Ueno and K. Kasono (unpublished).

¹⁷J. L. Cardy, J. Phys. A **13**, 1507 (1980).

¹⁸Y. Ueno and Y. Ozeki, J. Stat. Phys. **64**, 277 (1991).

¹⁹K. Okamoto and Y. Ueno (unpublished).

²⁰For example, see *Phase Transitions and Critical Phenomena*, edited by C. Domb and J. L. Lebowitz (Academic, New York, 1984), Vol. 10.

²¹M. E. Fisher, in *Critical Phenomena*, Proceedings of the 51st Enrico Fermi Summer School, Course 51, edited by M. S. Green (Academic, New York, 1971), p. 1; M. N. Barber, *Phase Transitions and Critical Phenomena*, edited by C. Domb and J. L. Lebowitz (Academic, New York, 1984), Vol. 9, p. 145.

²²V. Privman and M. E. Fisher, Phys. Rev. B **30**, 322 (1984); V. Privman, P. C. Hohenberg, and A. Aharony, in *Phase Transitions and Critical Phenomena*, edited by C. Domb and J. L. Lebowitz (Academic, New York, 1992), Vol. 14, p. 1.

²³In case of the IOP1, $\psi_{\alpha\beta}$ becomes negative or positive depending on $\alpha\beta$, which gives important properties of the IOP1, as seen later in this paper.

²⁴K. Binder, *Application of the Monte Carlo Method in Statistical Physics*, edited by K. Binder (Springer, Heidelberg, 1987), p. 1.

²⁵See, for example, P. G. de Gennes and C. Taupin, J. Phys. Chem. **86**, 2294 (1982).

²⁶M. D'Onorio De Meo, D. W. Heermann, and K. Binder, J. Stat. Phys. **60**, 585 (1990).

²⁷T. Satomura, Master thesis, Tokyo Institute of Technology, 1993; T. Satomura and Y. Ueno (unpublished).

²⁸A. N. Berker and D. Andelman, J. Appl. Phys. **53**, 7923 (1982).

²⁹K. Kihara, T. Mizuno, and J. Shizume, J. Phys. Soc. Jpn. **9**, 681 (1951).

³⁰See, for example, L. Longa and A. M. Oleś, J. Phys. A **13**, 1031 (1980) for Ising frustrated models and Ref. 9 for layered Potts models.

³¹Y. Ueno (unpublished).

³²L. D. Landau and E. M. Lifshitz, *Statistical Physics* (Pergamon, London, 1959).